

Lifetime of fluorescent dye molecules in dense aqueous suspensions of polystyrene nanoparticles

Giuseppe Scalia and Frank Scheffold*

*Department of Physics and Fribourg Center for Nanomaterials, University of Fribourg,
CH-1700 Fribourg, Switzerland*

**Frank.Scheffold@unifr.ch*

Abstract: We study the lifetime of two common fluorescent dye molecules from the Alexa Fluor NHS Ester family dissolved in water in an opaque aqueous dispersion of dielectric polystyrene nanoparticles. We investigate the role of the dispersion composition by varying the particle concentration and adding SDS (sodium dodecyl sulfate) surfactant molecules. The observed strong changes in lifetime of Alexa 430 can be attributed to the relative contribution of radiative and non-radiative decay channels while the lifetime of the Alexa 488 dye depends only weakly on the sample composition. For Alexa 430, a dye with a rather low quantum yield in aqueous solution, the addition of polystyrene nanoparticles leads to a significant enhancement in quantum yield and an associated increase of the fluorescent lifetime by up to 55 %. We speculate that the increased quantum yield can be attributed to the hydrophobic effect on the structure of water in the boundary layer around the polystyrene particles in suspension. Adding SDS acts as a quencher. Over a range of particle concentrations the particle induced increase of the lifetime can be completely compensated by adding SDS.

© 2015 Optical Society of America

OCIS codes: (260.2510) Fluorescence; (290.5850) Scattering, particles; (290.7050) Turbid media; (350.4238) Nanophotonics and photonic crystals; (240.6670) Surface photochemistry; (180.2520) Fluorescence microscopy.

References and links

1. O. Painter, R. Lee, A. Scherer, A. Yariv, J. O'Brien, P. Dapkus, and I. Kim, "Two-dimensional photonic band-gap defect mode laser," *Science* **284**, 1819–1821 (1999).
2. P. Michler, A. Kiraz, C. Becher, W. Schoenfeld, P. Petroff, L. Zhang, E. Hu, and A. Imamoglu, "A quantum dot single-photon turnstile device," *Science* **290**, 2282–2285 (2000).
3. B. O'regan and M. Grätzel, "A low-cost, high-efficiency solar cell based on dye-sensitized colloidal TiO_2 films," *Nature (London)* **353**, 737–740 (1991).
4. M. Sauer, J. Hofkens, and J. Enderlein, *Handbook of Fluorescence Spectroscopy and Imaging: From Ensemble to Single Molecules* (John Wiley & Sons, 2010).
5. B. Kolaric, K. Baert, M. Van der Auweraer, R. A. Vallée, and K. Clays, "Controlling the fluorescence resonant energy transfer by photonic crystal band gap engineering," *Chem. Mater.* **19**, 5547–5552 (2007).
6. K. Vynck, M. Burresi, F. Riboli, and D. S. Wiersma, "Photon management in two-dimensional disordered media," *Nature materials* **11**, 1017–1022 (2012).
7. H. A. Al Attar and A. P. Monkman, "FRET and competing processes between conjugated polymer and dye substituted dna strands: A comparative study of probe selection in dna detection," *Biomacromolecules* **10**, 1077–1083 (2009).

8. W. Stöber, A. Fink, and E. Bohn, "Controlled growth of monodisperse silica spheres in the micron size range," *J. Colloid Interf. Sci.* **26**, 62–69 (1968).
9. N. Panchuk-Voloshina, R. P. Haugland, J. Bishop-Stewart, M. K. Bhalgat, P. J. Millard, F. Mao, W.-Y. Leung, and R. P. Haugland, "Alexa dyes, a series of new fluorescent dyes that yield exceptionally bright, photostable conjugates," *J. Histochem. Cytochem.* **47**, 1179–1188 (1999).
10. B. Tong, Y. Liu, S. Wong, P. John, Y.-t. Zhu, and W. Ware, "Fluorescence-lifetime measurements in monodispersed suspensions of polystyrene particles," *J. Opt. Soc. Am. B* **10**, 356–359 (1993).
11. W. Becker, *The bh TCSPC Handbook* (Becker & Hickl, 2008).
12. D. R. Larson, H. Ow, H. D. Vishwasrao, A. A. Heikal, U. Wiesner, and W. W. Webb, "Silica nanoparticle architecture determines radiative properties of encapsulated fluorophores," *Chem. Mater.* **20**, 2677–2684 (2008).
13. K. B. Lee, J. Siegel, S. Webb, S. Leveque-Fort, M. Cole, R. Jones, K. Dowling, M. Lever, and P. French, "Application of the stretched exponential function to fluorescence lifetime imaging," *Biophys. J.* **81**, 1265–1274 (2001).
14. K. Drexhage, "Influence of a dielectric interface on fluorescence decay time," *J. Lumin.* **1**, 693–701 (1970).
15. D. Toptygin, R. S. Savtchenko, N. D. Meadow, S. Roseman, and L. Brand, "Effect of the solvent refractive index on the excited-state lifetime of a single tryptophan residue in a protein," *J. Phys. Chem. B* **106**, 3724–3734 (2002).
16. D. Magde, R. Wong, and P. G. Seybold, "Fluorescence quantum yields and their relation to lifetimes of rhodamine 6g and fluorescein in nine solvents: Improved absolute standards for quantum yields," *Photochem. Photobiol.* **75**, 327–334 (2002).
17. J. J. Sakurai and S. F. Tuan, *Modern quantum mechanics*, (Addison-Wesley Reading, 1985), Vol. I.
18. R. Chance, A. Prock, and R. Sylbey, "Molecular fluorescence and energy transfer near interfaces," *Adv. Chem. Phys.* **37**, 65 (1978).
19. R. X. Bian, R. C. Dunn, X. S. Xie, and P. Leung, "Single molecule emission characteristics in near-field microscopy," *Phys. Rev. Lett.* **75**, 4772 (1995).
20. S. Kühn, U. Håkanson, L. Rogobete, and V. Sandoghdar, "Enhancement of single-molecule fluorescence using a gold nanoparticle as an optical nanoantenna," *Phys. Rev. Lett.* **97**, 017402 (2006).
21. P. Anger, P. Bharadwaj, and L. Novotny, "Enhancement and quenching of single-molecule fluorescence," *Phys. Rev. Lett.* **96**, 113002 (2006).
22. J. D. Joannopoulos, S. G. Johnson, J. N. Winn, and R. D. Meade, *Photonic crystals: molding the flow of light* (Princeton University Press, 2011).
23. M. R. Jorgensen, J. W. Galusha, and M. H. Bartl, "Strongly modified spontaneous emission rates in diamond-structured photonic crystals," *Phys. Rev. Lett.* **107**, 143902 (2011).
24. M. Leistikow, A. Mosk, E. Yeganeh, S. Huisman, A. Lagendijk, and W. Vos, "Inhibited spontaneous emission of quantum dots observed in a 3d photonic band gap," *Phys. Rev. Lett.* **107**, 193903 (2011).
25. D. Toptygin, "Effects of the solvent refractive index and its dispersion on the radiative decay rate and extinction coefficient of a fluorescent solute," *J. Fluoresc.* **13**, 201–219 (2003).
26. A. H. Sihvola, *Electromagnetic mixing formulas and applications*, Vol. XLVII (Iet, 1999).
27. J. Martorell and N. Lawandy, "Spontaneous emission in a disordered dielectric medium," *Phys. Rev. Lett.* **66**, 887 (1991).
28. L. Froufe-Pérez, R. Carminati, and J. Sáenz, "Fluorescence decay rate statistics of a single molecule in a disordered cluster of nanoparticles," *Phys. Rev. A* **76**, 013835 (2007).
29. M. Birowosuto, S. Skipetrov, W. Vos, and A. Mosk, "Observation of spatial fluctuations of the local density of states in random photonic media," *Phys. Rev. Lett.* **105**, 013904 (2010).
30. R. Sapienza, P. Bondareff, R. Pierrat, B. Habert, R. Carminati, and N. Van Hulst, "Long-tail statistics of the purcell factor in disordered media driven by near-field interactions," *Phys. Rev. Lett.* **106**, 163902 (2011).
31. L. F. Rojas-Ochoa, J. Mendez-Alcaraz, J. Sáenz, P. Schurtenberger, and F. Scheffold, "Photonic properties of strongly correlated colloidal liquids," *Phys. Rev. Lett.* **93**, 073903 (2004).
32. Thermo Fisher, "Alexa Fluor NHS Ester product manual," <https://tools.thermofisher.com/content/sfs/manuals/>.
33. L. Rojas-Ochoa, S. Romer, F. Scheffold, and P. Schurtenberger, "Diffusing wave spectroscopy and small-angle neutron scattering from concentrated colloidal suspensions," *Phys. Rev. E* **65**, 051403 (2002).
34. P. Zakharov and L. Rojas-Ochoa, "Online Mie scattering calculator," <http://www.lsinstruments.ch/>.
35. Y. I. Tarasevich, "State and structure of water in vicinity of hydrophobic surfaces," *Colloid J.* **73**, 257–266 (2011).
36. A. Faghihnejad and H. Zeng, "Hydrophobic interactions between polymer surfaces: using polystyrene as a model system," *Soft Matter* **8**, 2746–2759 (2012).
37. I. Bischofberger, D. Calzolari, P. De Los Rios, I. Jelezarov, and V. Trappe, "Hydrophobic hydration of poly-n-isopropyl acrylamide: a matter of the mean energetic state of water," *Sci. Rep.* **4**, 4377 (2014).
38. P. Kumar and H. Bohidar, "Universal correlation between solvent polarity, fluorescence lifetime and macroscopic viscosity of alcohol solutions," *J. Fluoresc.* **22**, 865–870 (2012).
39. Due to the lower refractive index of the silica particles suspended in water the scattering mean free path is always larger than sample thickness both for the incident and the emission wavelength and over the range of particle concentrations studied [33, 34]. The light collection efficiency is thus not affected by multiple scattering of light.

1. Introduction

One of the most important questions in nano-optics and molecular imaging applications is how a point source (such as a fluorescent dye molecule) emits in a complex dielectric environment. This question lies at the heart of modern quantum optics and it is important for many applications ranging from laser technology [1] to single photon sources [2], solar cells [3] and all varieties of fluorescence spectroscopy and imaging microscopy [4]. A detailed understanding of this question is of paramount importance in the development of molecular imaging techniques in life sciences. For example FLIM (fluorescence lifetime imaging microscopy) exploits the fact that a fluorescent molecule has a different lifetime depending on its dielectric environment [4]. Moreover, by an appropriate design of the microenvironment, it will be possible to tune photon states in order to enhance or filter photonic signals. Tailoring the local density of states can for example be used to shape the absorption and emission spectrum of a fluorophore or to enhance fluorescence resonant energy transfer (FRET) by photonic band gap engineering as shown in [5, 6]. Understanding the fluorescent decay in a complex and well controlled dielectric environment is therefore of great importance.

In the present work we study the lifetime of two common fluorescent dye molecules from the Alexa Fluor NHS Ester family dissolved in water in an opaque aqueous dispersion of dielectric polystyrene nanoparticles. We investigate the role of the dispersion composition by varying the particle concentration and adding SDS (sodium dodecyl sulfate) surfactant molecules. Interestingly, we find a significant composition dependence of the fluorescent lifetime for only one of the dyes studied, namely Alexa 430, while the lifetime of the Alexa 488 dye depends only weakly on the sample composition. We show that the observed strong changes in lifetime of Alexa 430 can be attributed to the relative contribution of radiative and non-radiative decay channels. For Alexa 430, a dye with a rather low quantum yield in aqueous solution at neutral pH [7], the addition of particles leads to an increase in quantum yield which is associated with an increase of the fluorescent lifetime by a corresponding factor of approximately 1.5. We argue that the increased quantum yield can be attributed to the boundary layer around the hydrophobic polystyrene particles in suspension. Adding SDS acts as a quencher. Over a range of particle concentrations the particle induced increase of the lifetime can be completely compensated by adding SDS.

2. Materials and Methods

We prepare a concentration series of polystyrene particles, diameter $2R = 130\text{nm}$, dispersed in water. The beads we use are commercially available surfactant free negatively charged polystyrene latex spheres (BangsLabs, USA), polydispersity 5%, and the concentrations is varied from 0.3 to 10 vol% in small steps. The particle refractive index is $n_p \simeq 1.59$ at the emission wavelength of $\lambda \sim 500\text{nm}$ and the refractive index of water is $n_s \simeq 1.33$. At these concentrations the samples appear translucent to highly opaque. As a control we also prepare suspensions of monodisperse negatively charged silica (SiO_2) particles (Microparticles GmbH, Germany), diameter 136 nm and polydispersity 3%, over the same concentration range [8]. We study the lifetime of two standard dye molecules from the Alexa Fluor family: Alexa Fluor 430 NHS Ester (succinimidyl ester) and Alexa Fluor 488 NHS Ester (Molecular Probes, Life Technologies, USA) [9]. Both dye molecules are anionic and are thus repelled from the surface of the nanoparticles. Alexa 430 shows an absorption maximum at $\lambda_a = 434\text{nm}$ and emission maximum at $\lambda_e = 541\text{nm}$. Alexa 488 shows an absorption maximum at $\lambda_a = 495\text{nm}$ and emission maximum at $\lambda_e = 519\text{nm}$. We set the dye concentration such that the ratio between particles and dye molecules is 1 : 10 at two reference points $\phi = 5\%$ ($N/V = 5.53 \times 10^{14}/\text{cm}^3 \simeq 1\mu\text{mol}$) and $\phi = 10\%$ ($N/V = 11.06 \times 10^{14}/\text{cm}^3 \simeq 2\mu\text{mol}$) where N denotes the number density of the dye molecules. The dye concentration is chosen sufficiently low to avoid repeated reabsorption and

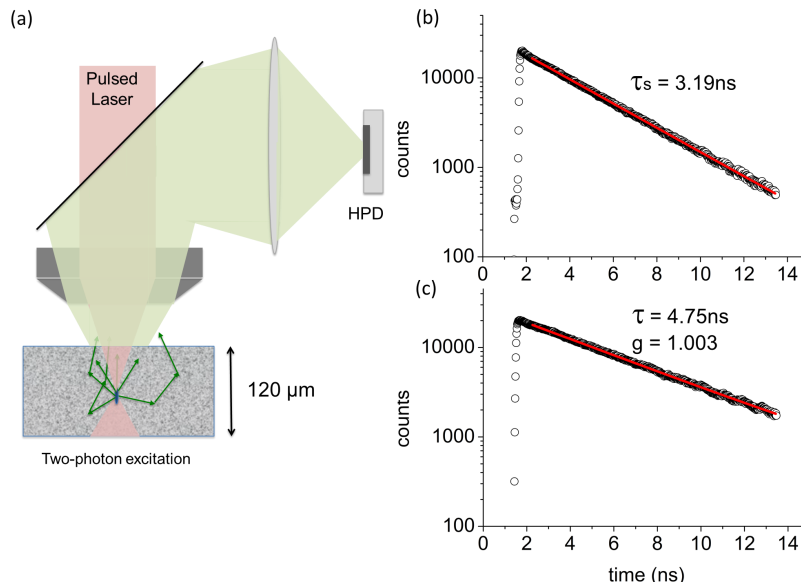


Fig. 1. (a) Sketch of the experimental setup. The lifetime of the dye molecules in a concentrated suspensions of dielectric particles is determined using a custom made two-photon microscope setup combined with a time correlated single photon counting (TCSPC) board. The near infrared fs pulsed laser light $\lambda_L \sim 900\text{nm}$ is focused inside the sample and the emitted fluorescence is detected using a hybrid photo-detector module (HPD). (b) Time-resolved fluorescence of the dye Alexa 430 dissolved in water at neutral pH (decay time in the pure solvent $\tau_s = 3.19\text{ns}$) (c) Time-resolved fluorescence of the dye Alexa 430 in a suspension of polystyrene particle concentration of $\phi = 4.8\%$ (decay time $\tau = 4.75\text{ns}$). The acquisition time has been set to 60s in both cases. The TCSPC data is fitted with a stretched exponential function ($F(t) = F_0 + Ae^{-(t/\tau)^g}$) to verify that the decay is single exponential.

emission which might otherwise influence the measured lifetime [10]. Moreover the spectral overlap between emission and absorption is low for Alexa 430, which is the more interesting dye studied in this work.

We dilute the stock suspension with aqueous dye solution keeping the dye concentration constant between $0 < \phi \leq 5\%$ and $1\% < \phi < 10\%$. All measurements are performed at neutral $\text{pH} \simeq 7.2$. For the Alexa 430 dye we also study the influence of adding controlled amounts of the common surfactant SDS. For the other dye, Alexa 488, the addition of SDS does not show any detectable influence on the lifetime. We have verified that the decay characteristics of both dyes in suspension remain unaffected by the addition of 1 mM NaCl. This is an important result as it shows that screening correlations and interactions between the negatively charged dyes and the equally charged colloidal particles does not influence the results reported here. The samples are contained between two coverslips sealed with an imaging spacer (Secure Seal imaging spacer, Grace Bio-Labs Inc.) of 120 μm thickness. Both dyes are excited via two photon absorption with a Coherent Mira 900 fs laser system operating at a mean wavelength of $\lambda_L \simeq 900\text{nm}$ and a 80MHz repetition rate. The laser pulses are focused with an Olympus XLUMPlanFI 20X objective (NA=0.95) 50 μm below the glass surface. The emitted epifluorescence light is collected via a dichroic mirror followed by a heat-protection filter (Calflex-CTM, QiOptiq Photonics SAS) to remove the bleed-through of IR excitation light. We then select the emission wavelength of the dye with a set of emission filters (543/22 nm BrightLine single-band

bandpass filter, 520/35 nm BrightLine single-band bandpass filter Semrock Inc.) and a relay optics is used to focus the light onto an after-pulsing free hybrid-single photon detector (HPM 100-40 Becker & Hickl, Germany). The decay time is recorded using a time correlated single photon counting (TCSPC) PCI-board (SPC-150, Becker & Hickl, Germany). The accessible time window for the TCSPC is limited to 12.5ns by the repetition rate of the fs-pulsed laser (80MHz). The excitation power for each series of measurements at constant dye concentrations is set after scanning the emitted fluorescence intensity for increasing laser powers, in order to avoid saturation effects. A sketch of the experimental setup is shown in Fig. 1(a). In Fig. 1(b) and Fig. 1(c) we show the change of fluorescent lifetime for the Alexa 430 dye molecules without and with the addition of the polystyrene spheres (at a concentration of $\phi = 4.8\%$). For a given dye concentration all the measurements are performed with the same acquisition parameters (Time to Amplitude Converter (TAC) gain and range, acquisition time) and the same laser power. To avoid effects due to fluorescence depolarization of the dye, the polarization plane of the excitation laser is oriented 45° from the vertical plane. With the laser at 45° the detection efficiency for the two components of the emitted fluorescence, parallel and orthogonal, is almost balanced and thus our measurements approximately yield the decay function for unpolarized illumination [11].

The measured time-resolved data $F(t)$ from each sample correspond to the convolution of the intrinsic fluorescence signal $S(t)$ with the internal response function $IRF(t)$: $F(t) = S(t) * IRF(t)$. The internal response function $IRF(t)$ represents the distortions in the detected time-resolved dynamics due to the response of the electronics, the optics, and the finite temporal profile of the excitation pulse. The internal response function is obtained by measuring independently the decay curve from two different strongly scattering suspensions (polystyrene microspheres, diameter 130 nm, at volume fraction $\phi = 10\%$ and silica microspheres, diameter 136nm at $\phi = 12\%$) replacing the emission band pass filter with an ND filter, to attenuate the light intensity detected by the HPD. The fluorescence decay data are fitted using two different methods. We first use the decay fitting software of the TCSPC card (SPCImage v.4.9, Becker & Hickl, Germany) to extract the decay time τ (see also [12]). We then compare the fluorescence lifetime data with a custom made fitting routine that corrects for background and the contribution of the internal response function. To this end the experimental data is fitted using a stretched exponential function $F(t) = F_0 + Ae^{-(t/\tau)^g}$. Here the parameter g allows us to see whether or not the decays are single exponential [13]. Both fitting approaches give the same results within the experimental error of a few per cent.

3. Results

For the Alexa 488 dye we observe only a small influence of the dispersed particles as shown in Fig. 2(a): the lifetime decreases monotonically by a few per cent with increasing concentration up to 10%. For the Alexa 430 however the lifetime displays a rich dependence on both particle concentration and on the addition of SDS surfactant. We also verified for all cases that the dye molecules do not irreversibly adsorb to the particle surface by spinning down the particles in a centrifuge and measuring the intensity and lifetime in the supernatant and the sediment. This is an important result as it shows that in our experiments the dye does not attach to the particle surface as it was claimed to be the case [10] in the context of a previous study of lifetime measurements in polystyrene nanoparticle suspensions using the anionic dye Kiton Red S.

In the absence of SDS the lifetime increases and asymptotically reaches a constant value, Fig. 2(a). Adding SDS to moderately dense dispersion acts as a quencher and drives the lifetime back towards the initial state as shown in Fig. 3. For a fixed SDS concentration the curve is thus shifted and the onset of the lifetime-increase is delayed. In both case the initial increase is linear and then saturates at $\tau_{max}/\tau_s \sim 1.55$. Overall the transition from the linear to the sat-

urated regime is well described by a hyperbolic tan-function. We note that the results for the two different dye concentrations perfectly collapse on the same curve which confirms that contributions due to reabsorption and remission are negligible for Alexa 430. In Fig. 2(b) we report the measured count rates I normalized by the count rate of the dye in pure water I_s . In general, a quantitative analysis and interpretation of the count rate is more difficult due to the increased noise and the varying levels of background. Moreover we are not able to quantitatively predict the changes in collection efficiency due to scattering and the possible differences related to the exact positioning of the sample. Nonetheless we observe that the count rate measurements Fig. 2(b) follow a very similar trend as compared to the lifetime measurements shown in Fig. 2(a). The concentration dependence for the case of Alexa 488 is weak whereas the count rate increases substantially for Alexa 430.

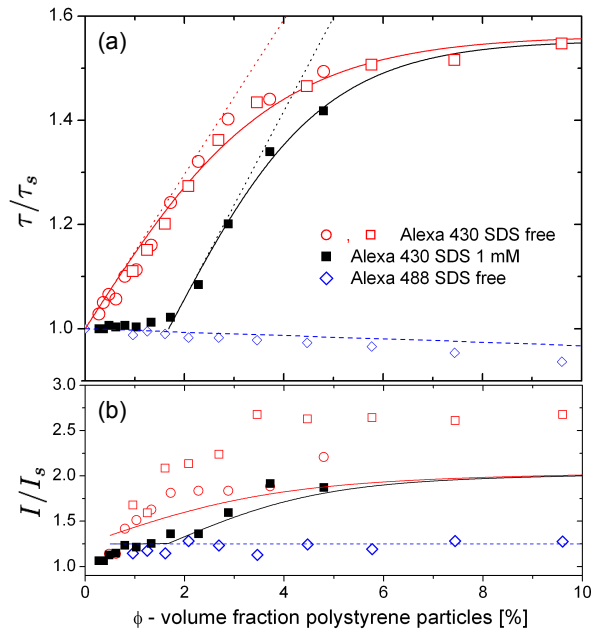


Fig. 2. (a) Measured lifetime normalized to value in pure water (Alexa 488: $\tau_s = 4.1\text{ns}$, Alexa 430: $\tau_s = 3.19\text{ns}$) for different sample compositions. The solid lines are empirical fits to the data with $\tau(\phi)/\tau_s = a \cdot \tanh[(\phi - \phi_0)/w] + 1$, $a = \tau_{max}/\tau_s - 1$. Alexa 430 SDS free: $a = 0.56$, $w = 3.8\%$ and $\phi_0 = 0$, Alexa 430 SDS 1mM: $a = 0.55$, $w = 3.07\%$ and $\phi_0 = 1.68\%$. The dotted lines show the linear expansion of the fit $\tau(\phi)/\tau_s \simeq 1 + (a/w)\phi$ at low concentrations. The dashed line is derived from the empty spherical cavity (ESC) model as explained in the text. (b) Measured count rates I normalized to value in pure water I_s for the same samples as in (a). Solids lines are calculated from $I(\phi)/I_s = 1.25 \cdot \eta(\phi)/\eta_s$ (for details see text).

4. Discussion

Our experiments show that two common dyes can react differently to the addition of scattering dielectric polystyrene particles and SDS although other parameters are kept unchanged. For an interpretation of the observed behavior we first recall the mechanism that may influence the decay rate of a dye molecule from an excited to a relaxed state via radiative and non-radiative pathways. The relative importance of non-radiative processes can be measured by the decrease

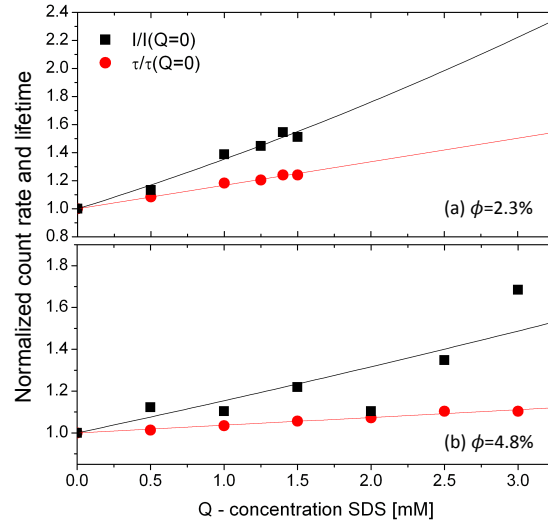


Fig. 3. Quenching of fluorescence by adding SDS dye solutions at two different nanoparticle concentrations ϕ . Relative changes in fluorescent count rates (full squares) and lifetimes (full circles) of Alexa 430 fluorophores. Solid lines: Eq.(4) and Eq.(5) for (a) $\phi = 2.3\%$ with quenching constants $K_d = 0.17 \text{ mM}^{-1}$ and $K_s = 0.16 \text{ mM}^{-1}$ and (b) $\phi = 4.8\%$ with quenching constants $K_d = 0.037 \text{ mM}^{-1}$ and $K_s = 0.11 \text{ mM}^{-1}$.

in the quantum yield η . The fluorescence quantum yield η of a dye molecule is defined by the ratio of the emitted photons and the absorbed photons. We can also express it as a function of the decay rates Γ : [14, 15]

$$\eta = \Gamma_r / (\Gamma_r + \Gamma_{nr}) \quad (1)$$

In practice the actual relaxation of a single molecule embedded in medium results from both radiative and non-radiative process:

$$\tau_f = 1 / (\Gamma_r + \Gamma_{nr}) \quad (2)$$

The quantum yield tends towards one as the non-radiative decay rate tends zero [16]. We can express the measured lifetime as follows:

$$\tau_f = \eta \Gamma_r^{-1} \quad (3)$$

Changes in the fluorescent lifetime are often associated with changes in the non-radiative decay rate and thus the quantum yield. Indeed the local environment can profoundly alter the availability of non-radiative decay pathways. This can be easily seen in Fig. 3 where the addition of SDS molecules acts as a quencher. A well-known quenching mechanism upon the addition of molecules is the so called collisional quenching. Through diffusive encounters the fluorophore is returned to its ground state as a non-radiative decay pathway (dynamic quenching). A competing mechanism is the inactivation of the fluorophore by complex formation with the quencher molecule (static quenching). The probability for both is proportional to the concentration of added quencher molecules. Since the lifetime only depends on dynamic quenching both processes can be distinguished by analyzing the lifetime and the measured count rate:

$$\frac{I_{Q=0}}{I(Q)} = [1 + K_d \cdot [Q]] + [1 + K_s \cdot [Q]] \quad (4)$$

$$\frac{\tau_{Q=0}}{\tau(Q)} = [1 + K_d \cdot [Q]] \quad (5)$$

,where K_d is the dynamic and K_s the static quenching constant. $[Q]$ is the concentration of SDS. Our results show that SDS acts as a mixed static and dynamic quencher with quenching constants given in the caption of Fig. 3.

We now return to the discussion of fluorescent lifetime in the SDS-free suspensions. While the dependence of the radiative decay rate Γ_r to the local environment of an excited emitter are often small, they can, in some particular cases, become very important. On a fundamental level the link between the quantum emission process and the environment is established via Fermi's golden rule which states that the transition probability, or the radiative decay rate Γ_r , is directly proportional to the local density of final states (LDOS) at the emitted photon energy $h\nu$ [17]. Dielectric or metal structures under resonant conditions thus can efficiently suppress or enhance the emission rate [14, 18, 19]. The influence of well-defined geometrical structures on the decay rate has been studied in detail over the last decades addressing the situation for single emitters near metallic surfaces, close to tips or nanoantennas [18–21]. In some cases the radiative decay rate can even become zero, such as for example inside a full gap of a photonic crystal [22–24].

In the absence of resonant *plasmonic* or *photonic* effects changes in the radiative decay rate are continuous and can be expressed in terms of a single parameter, the refractive index n of the dielectric environment. To establish a basis for the further discussion we first analyze this contribution to changes of the decay time, which, as we will see, is relatively small. Different theoretical models have been suggested and a comprehensive review and discussion can be found in ref. [25]. Here we apply the empty spherical cavity model (ESC) for dipolar emission which should be a fairly good approximation for our case. The basic idea is to place the emitter in a small empty volume and solve the respective equations (Fermi's golden rule) for the emission into a dielectric with refractive index n (for details see [25]). The model predicts

$$\Gamma_r = (3n^2)^2 / (2n^2 + 1)^2 n \Gamma_0 \quad (6)$$

,where Γ_0 is the radiative decay rate in vacuum ($n=1$) also called the *natural* decay rate. From Eq. (6) we conclude that an increase of the refractive index always leads to an increase of Γ_r or a decrease of τ . For example when the refractive index changes from $n = 1.33$ (water) to $n = 1.4$ the lifetime is expected to decrease by a mere 9%, a relatively modest effect. It is thus obvious that the ESC-model can only describe one of the experimental data sets shown in Fig. 2. Indeed Eq. (6) is found in fairly good agreement with the experimental data for Alexa 488 if we assume a mean refractive index of the dispersion given by the Bruggemann mixing rule [26]. The refractive index of the polystyrene particles is $n_{PS} = 1.59$ and the refractive index of water $n_{H_2O} = 1.33$. The decrease of the fluorescent lifetime in Alex 488 can thus be explained by a trivial increase of the effective refractive index of the surrounding dielectric material.

In this context it is worth to recall again that the strong multiple scattering of light renders the dispersion highly opaque. It has been claimed that in this regime the electric field radiated by the dye molecules and the scattered field from the dielectric spheres interfere leading to significant oscillations of $\tau(\phi)$ as reported in the work from Martorell and Lawandy from 1991 [27]. However, the validity of these results has been questioned in [10]. Although the optical properties, particle size and density are comparable in our experiments we do not observe any evidence for such an effect. Moreover recent theoretical and experimental studies suggest that a much higher refractive index contrast is needed to induce interference effects on the fluorescent lifetime [28–31]. Our most strongly scattering sample has a particle volume fraction of about 10%. The scattering mean free path of this rather dense sample is $l \simeq 40\mu\text{m}$ and thus

$kl \simeq 630$ as calculated from Mie theory for an emission wavelength of $\lambda \simeq 530\text{nm}$ and a corresponding wavenumber (in water) $k = 2\pi n_s/\lambda = 15.8/\mu\text{m}$ [34]. Therefore, in our samples, kl is always more than one order of magnitude larger than for the *weak scattering* case ($kl \simeq 24$) studied in reference [30] for a solid sample. For the latter case a distribution of decay rates with a standard deviation of approximately 11% has been reported. In our experiments we record an ensemble average of decay rates in a liquid environment and due to the limited dynamic range of our experiment (see Fig. 1) we are not able to detect the small effect on the stretching parameter g that could be associated with a narrow distribution of lifetimes.

The question remains: what are the underlying mechanisms leading to the strong increase of the lifetime for the case of Alexa 430 while the lifetime of Alexa 488 depends only weakly on the particle concentration? Both dyes are carboxylic acid (negatively charged), succinimidyl esters and amine reactive that hydrolyze into the nonreactive free acid in aqueous solutions [32]. However, the two dyes differ markedly in their fluorescence quantum yield. While Alexa 488 has an approximate quantum yield of nearly 100% in pure water at neutral pH, the quantum yield of Alexa 430 is only about 65% [4, 7, 9]. This strongly suggests that the addition of the particles lead to an increase in quantum yield for the Alexa 430 emission. We can estimate an upper limit for such an increase based on Eq. (4). If we assume that Γ_r^{-1} remains constant and $\eta_s \simeq 0.65 \rightarrow \eta_{max} = 1$ we expect a maximal increase of the lifetime by a factor 1.55. This value exactly matches the observed increase in the lifetime τ . The accompanying increase in the measured count rate is a bit more pronounced than expected from $I/I_s \simeq \eta/\eta_s$ (see also Eq. (4)) but this additional enhancement can be attributed, at least partly, to changes in collection efficiency of the emitted light due to scattering. In a turbid sample a significant amount of scattered light, not captured directly by the imaging the focal volume, can still be collected. As matter of fact we observe an initial increase of the count rates for all data sets by about 25% as the sample becomes highly turbid already at low concentrations. From a Mie scattering calculation we find that the scattering mean free path ($l_s \sim 1/\phi$) for the emitted light l_s drops below the sample cell thickness for concentrations above 2% [33, 34]. We thus expect the collection efficiency to increase quickly and then to saturate for $\phi > 2\%$. We also note that scattering losses in the incident NIR beam are negligible since the scattering length in this spectral range is always large compared to the depth of the focal plane. The subsequent increase is fairly well described by $I(\phi)/I_s = 1.25 \cdot \eta(\phi)/\eta_s$, as shown in Fig. 2(b), although some discrepancies remain for the SDS free case. Here we have calculated the quantum yield $\eta(\phi)$ from Eq. (4) using the experimental data for $\tau_f(\phi)$ and Γ_r^{-1} from Eq. (6). From the previous discussion we can conclude that changes in lifetime are controlled by a (small) change of the radiative decay rate due to change of the average refractive index and a substantial change of the quantum yield η of Alexa 430 upon the addition of polystyrene particles.

Next we address in more detail the role played by the polystyrene particles. As shown in Fig. 2 the initial increase of the lifetime scales linearly with the particle concentration of $\tau(\phi) \sim \phi$. Since the particles are very large compared to the dye molecules we have to consider interactions between the molecules and the particle surface. To this end we can attribute a corona of thickness d to each particle, a sketched in Fig. 4. Dye molecules within this corona are sufficiently close and will be influenced by the vicinity to the particle surface. We assume that the lifetime scales with the part of the total sample volume ϕ affected and we can write $\tau(\phi)/\tau_s = 1 + \varphi(\phi)(\tau_{max}/\tau_s - 1)$. For simplicity we neglect the volume occupied by the particles themselves in the limit $\phi \ll \varphi$ and obtain $\varphi(\phi) = \phi(1 + d/R)^3$. By comparison with the fit shown in Fig. 2(a) we can immediately identify $\tau(\phi)/\tau_s \simeq 1 + (a/w)\phi$ and thus $1/w = (1 + d/R)^3 \simeq 26.3$ and therefore $d \simeq 2R \simeq 130\text{nm}$. For large concentrations the corona of different particles overlap and thus for $\phi > w$ the quantum yield and lifetime saturate. In principle, based on this model, one would expect that different dye populations contribute to a

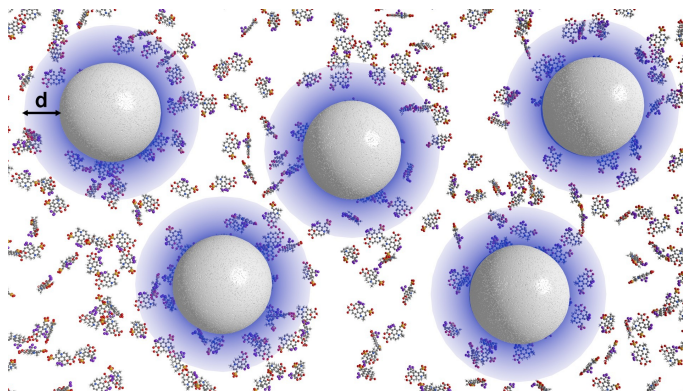


Fig. 4. The fluorescent properties of dye molecules located in the vicinity of hydrophobic polystyrene particles are modified leading to an increased quantum efficiency η . The sketch shows the polystyrene particle and the shaded corona of thickness d as an indication for the effective range of the hydrophobic interactions. The dye molecules are shown as the small objects. At high particle densities the coronas will overlap and the increase in η saturates as observed in the experiment, Fig. 2.

spectrum of decay times leading to a stretched-exponential decay. In the experiment however we always observe a nearly single exponential decay with a stretching exponent $g = 1 \pm 0.01$. We have thus simulated the effect of a double exponential decay with τ_1 and $\tau_2 = 1.5\tau_1$ as well as a continuous distribution between τ_1 and τ_2 . Indeed we find that, over the limited range accessible in our experiment, we cannot resolve the contribution of the two relaxation processes within experimental error.

The mechanism for the strong and long range interactions between the polystyrene particle surface and the dye molecule, we speculate, can be attributed to the hydrophobic effect. As mentioned earlier we have verified that the dye molecules do not adsorb to the particle surface. As a consequence the observed change in lifetime has to be mediated by the solvent, in the SDS free case pure water. Hydrophobic interfaces are known to have a strong influence on the state and structure of water in a boundary layer of several tens of nanometers. Tarasevich et al. have reported a more ordered layer of 35nm thickness close to a hydrophobic surface (carbon black) from X-ray scattering and neutron reflection methods [35]. Equally Faghihnejad and Zeng have reported surface force apparatus (SFA) measurements of long range interaction forces between hydrophobic surfaces in water extended up to several tens of nanometers [36]. The hydrophobic effect leads to structuring of water close to the polystyrene surface and thus reduces the orientation polarizability of water. In turn non-radiative decay pathways might become suppressed. A similar order-making mechanism in water is the addition of so-called kosmotropes, for example ethanol and methanol [37]. A recent study by Kumar and Bohidar has shown that the addition of small amounts of ethanol can lead to a substantial increase of the fluorescent lifetime of carbon nanoparticles [38]. This shows that the structure of an aqueous solvent can have a sizeable influence on the fluorescent lifetime. However, we also recognise that the corona of influence $d \sim 130\text{nm}$ appears to be rather long ranged compared to previous observations of water structuring close to a hydrophobic surface. A more quantitative modelling of the mechanism leading to the increase of the fluorescent lifetime of Alexa 430, however, is beyond the scope of this work.

Finally, in order to exclude other possible contributions, we have carried out a control experiment substituting the strongly hydrophobic polystyrene by silica (SiO_2), diameter 136 nm,

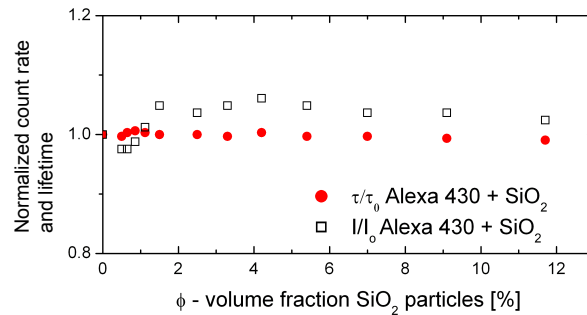


Fig. 5. Measured lifetime and emission count rate of Alexa 430 in aqueous dispersion of silica (SiO_2) colloidal particles. The plotted values are normalized by the value obtained in pure water.

which is hydrophilic due to the surface termination with silanols, or silicon-bonded hydroxyl groups, capable of forming hydrogen bonds with water molecules. As shown in Fig. 5 both the lifetime and the measured count rate are basically unaffected by the addition of silica particles. This provides further evidence that the observed behavior can likely be attributed to the hydrophobic structuring of water close to the polystyrene surfaces [39].

5. Summary and conclusion

In the present work we have analyzed the influence of polystyrene nanoparticles in suspension on the decay rate of dissolved dye molecules. Our work highlights the fact that such small particles expose a huge surface area and therefore, even for relatively small volume fractions, most or all of the dye molecules in solution can be within a close distance to the particles. The proximity of nanoparticles can then have a profound influence on the decay characteristics of the dye molecules, as we show in this work. Our results suggest that the strongly hydrophobic polystyrene surfaces provide a mechanism to inhibit non-radiative decay channels leading to an increase of the quantum yield and lifetime of the dye molecules. This scenario is further corroborated by the fact that the addition of hydrophilic silica particles of similar size does not show this effect. Moreover, recent studies of another structure forming mechanism have equally found an increase in the fluorescent lifetime of carbon nanoparticles suspended in water when adding small amounts of the kosmotrope ethanol [38].

Finally, our results also show that the influence of the dielectric particles on the radiative decay rate due to scattering and interference is weak for nanoparticles with a moderate refractive index contrast such as the polystyrene particles studied in this work. This conclusion is also supported by recent theoretical and experimental work that shows that changes to the radiative decay require a very high particle refractive index and/or the presence of a (nearly) full photonic band gap, conditions that are neither fulfilled in our work nor in a previous study claiming the opposite [27], both carried out with suspensions of polystyrene nanoparticles ($n = 1.59$) of comparable size suspended in water ($n = 1.33$).

Acknowledgments

We would like to acknowledge financial support by the Adolphe Merkle Foundations, the Systems X initiative (iPhD grant No. 2010/075 and RTD SynaptiX) and the Swiss National Science Foundation (grant No. 132736 and 149867). We thank Irmgard Bischofberger, Veronique Trappe and Luis Froufe-Pérez for interesting discussions and comments.